IEEE Access
Multidisciplinary | Rapid Review | Open Access Journal

Received January 16, 2020, accepted February 15, 2020, date of publication February 28, 2020, date of current version March 12, 2020.

Digital Object Identifier 10.1109/ACCESS.2020.2977258

Reliability-Based Safety Evaluation of Headlight Sight Distance Applied to Road Sag Curve Standards

F. ANDRADE-CATAÑO[1], C. DE SANTOS-BERBEL[2], AND M. CASTRO[1]
[1]Departamento de Ingeniería del Transporte, Territorio y Urbanismo, Universidad Politécnica de Madrid, 28040 Madrid, Spain
[2]Departamento de Estructuras y Física de Edificación, Universidad Politécnica de Madrid, 28040 Madrid, Spain

Corresponding author: M. Castro (maria.castro@upm.es)

This work was supported by the Spanish Ministerio de Economía y Competitividad, and the European Regional Development Fund (FEDER) under Grant TRA2015-63579-R (MINECO/FEDER).

ABSTRACT Sight distance is key to ensure safe road geometric design under all circumstances. Road design standards propose models simulating nighttime driving that contemplate the features of vehicle frontlighting systems to address the design of sag curves. These models are based on a deterministic approach, which is known to present a number of drawbacks. It neglects the stochastic nature of the variables involved and, therefore, no information is available about the safety margin of the design output. As opposed to design based on deterministic methods, probabilistic methods overcome these inconveniences providing a solid approach to broach the analysis of sag curves. This research study applied a probabilistic approach to evaluate the risk level (probability of noncompliance, P_{nc}) associated to sag curve designs, and assessed the effect of the variables involved in headlight sight distance (HSD) on the P_{nc}. The required stopping sight distance was considered not to be met when it exceeded the HSD. A total of 71,334 case studies were generated by combining the range of values of the variables involved in the HSD as per the Spanish geometric design standard. The risk level associated to each case was calculated by means of a Monte Carlo simulation. The results showed that variables modeling headlight features significantly affect the risk level. Moreover, the risk associated to design outputs that are considered equivalent by the standard varies significantly. Therefore, the use reliability theory in the development of standards and design guides is recommended.

INDEX TERMS Headlight sight distance, Monte Carlo simulation, reliability analysis, road geometric design, road safety, sag vertical curves.

I. INTRODUCTION

Sight distance is a factor of crucial importance to road geometric design. Its correct implementation in the road alignment allows the provisioning of the necessary space drivers need for performing different maneuvers such as passing or stopping.

When calculating sight distance, different environmental conditions must be considered, including sight distance at nighttime. This aspect can be corroborated by observing the significantly higher traffic accident frequency and severity in nighttime with respect to those that occurred in the day [1]. Despite the lower traffic intensity, 40% of fatalities occur at night [2]. The Spanish Directorate-General for Traffic (DGT) reported that 31% of fatalities occurred on Spanish roads in 2017 were at twilight or at night, including a 57% of pedestrians killed on interurban roads during these hours [3].

Given that the vehicle headlights represent the fundamental source of light at night on rural roads, the sight distance provided by the headlight beam is considered as the main criterion for determining sag vertical curve parameters. In addition, the explicit evaluation of the influence of uncertainty in decision-making, in the search of more efficient design outputs has been addressed in different investigations. The use of probabilistic design approaches that quantify risk and reliability have been successful in other disciplines and, when applied in road geometric design in research studies conducted recently, these have shown promising results.

The deterministic approach has two main shortcomings [4]. First, many variables of models on which design

The associate editor coordinating the review of this manuscript and approving it for publication was Yu Wang.

criteria are based are stochastic by nature. However, conservative percentile values are typically selected from their respective statistical distributions. Hence the safety margin of design outputs and, particularly, minimum standard requirements is unknown. Secondly, the implications of deviating from standardized values are unknown; therefore, both small and great deviations from these values are considered as unacceptable. The reliability theory accounts for the uncertainty of the model inputs and overcome the deficiencies associated with the deterministic approach [5].

This research study evaluated the potential effect of the geometric parameters involved in the estimation the headlight sight distance (HSD) on sag vertical curve design on road safety. In order to account for the model uncertainty, the reliability theory was used to calculate the probability of non-compliance (P_{nc}) associated to the design of sag vertical curves arranged according to the Spanish standard of geometric design [6]. In this sense, the combination of reliability theory and HSD for road safety assessment represents an area not studied so far.

In order to acknowledge and understand the different investigations that have contributed to the development of the topics related to this research, a literature review of the methodologies implemented of the headlamp and the reliability analysis of highway design was included in section II. The following section aims to explain the research in detail as well as the tools that led to the results. Moreover, a critical analysis of the results is included based on the research development. Finally, conclusions and future lines of research are given.

II. LITERATURE REVIEW

A. NIGHTTIME SIGHT DISTANCE AND ROAD DESIGN

The high accident rate at night with respect to the day evidences the hazard involved in driving in low light conditions since the reaction chances to road users are reduced [7]. A significantly higher relative risk has been found to exist during nighttime driving [8]. Gaca and Kiec [9] found an increase in rear-end collisions, in accidents involving side obstacles and accidents with pedestrians, from day to night conditions. Papadimitriou and Psarianos [10] stated that on two-lane rural roads with a potential risk of collision with wildlife, a speed reduction of at least 10 km/h at night is recommended. Lee and Kim [11] found that the obstacle color in nighttime determines the distance at which it is seen, and that the minimum headlight beam illumination level should be 5 lux. This highlights the importance of taking night conditions into account in road design.

Nighttime conditions in driving are incorporated into road geometric design to determine the layout of sag vertical curves through the HSD. The main geometric parameter that features sag curves is the rate of vertical curvature K_V. Bauer and Harwood found that reduced values of this parameter affect negatively safety performance, and quantified the impact of other alignment parameters on safety [12]. In addition, the nighttime condition criterion is typically based on a given value of the upward divergence angle of the headlight beam (α). Among the first identified references using this criterion, Noble et al. proposed an α value of 0.38 degrees, but it led to excessive curve lengths [13]. This research study was based on the evaluation of headlight performance carried out by Giessler [14]. In 1954, the American Association of State Highway Officials (AASHO) published a *Policy on Geometric Design of Rural Highways*, which incorporated the criterion of $\alpha = 1°$ [15]. It should be noted that this criterion has been maintained until the current edition of a *Policy on Geometric Design of Highways and Streets* [1]. Regarding the Spanish standard, which is what this study focuses on, an angle α of 1° is preserved for the design of sag vertical curves [6]. Considering developments in headlamp design, Gibbons *et al.* [16] found that the headlamps do not project enough light above its horizontal axis, to match the HSD calculated by considering an angle α of 1°. Hawkins and Gogula [17] evaluated the amount of light emitted by the headlamps above their horizontal plane. According to their results, a reduction in the α value from 1° to a value between 0.75° and 0.9° was proposed.

An alternative way to evaluate road geometric design in night conditions is to apply a 3D approach. Easa and Hassan [18] developed analytical models to calculate HSD for vertical and horizontal 2D alignments separately contemplating boundary conditions. These models were the basis for developing a methodology that determines the HSD on 3D, which they applied on vertical curves combined with horizontal curves [19]. Using a similar 3D procedure, De Santos-Berbel *et al.* [20] measured the effect of the headlight beam parameters on the HSD, finding that the angle α is the variable that affects HSD the most. In a further study considering swiveling frontlighting systems, the interaction between the swiveling angle and the boundary conditions was analyzed [21].

B. RELIABILITY THEORY APPLIED TO ROAD DESIGN

Reliability is defined as the probability that a system performs its intended function under operating conditions, for a specific period [22]. Current geometric design standards use a deterministic approach to establish the threshold values of alignment design parameters. This approach does not consider the uncertainty associated with many design parameters, and the safety margin of the design output is unknown. Therefore, a deterministic approach does not adequately represent the real performance of a system [23]. Reliability analysis is an alternative technique based on a probabilistic approach that seeks to overcome these inconveniences. In this sense, a better understanding of the variability and uncertainty in the design inputs and controls allows a more economical and efficient design of the road networks [24].

The reliability approach uses random variables instead of single value estimates as opposed to the deterministic approach. Design equations are represented by the limit state function (LSF), which is associated to a failure mode. The LSF evaluates the difference between supply (HSD) and demand (stopping sight distance, SSD)

(i.e. LSF = ASD-SSD). If the ASD is less than the SSD (LSF < 0), the design is considered to be failed or not complied with the requirements. Reliability theory is used to quantify the P_{nc} to assess whether the supply satisfies the demand in a particular design [25].

Several methods are available to determine the P_{nc} value, including the first and second order reliability methods (FORM / SORM), the mean-value first-order second-moment method (MVFOSM) and sampling methods.

MVFOSM uses the second moments of the random variables, i.e., means, standard deviations and correlation coefficients, to find the mean and standard deviation of the LSF. These two values determine the reliability index, which serves as a surrogate for P_{nc} value. FORM remedies the problems of other reliability methods, it being more efficient than sampling in terms of the number of iterations to determine P_{nc}. SORM is an extension of FORM but approximates LSF by a second order function. With regard to sampling methods, the Monte Carlo method has been extensively applied to system reliability analysis [26]. It relies on the repeated random sampling of the variables to obtain a numerical solution [27]. The precision of the solution depends on the number of iterations made [28].

Several studies have applied reliability analysis to geometric design problems. Navin [29] proposed a model to establish a safety factor and a reliability index in geometric design, similar to that used by structural engineers in buildings. This method was used to determine these factors in isolated components of a road, and validated the method in a SSD application [30].

Among the different reliability analysis methodologies, Richl and Sayed [31] applied the FORM and SORM to determine the risk associated to narrow medians combined with horizontal curves in stopping maneuvers using the Reliability Analysis Software (RELAN). Sarhan and Hassan [32] used the Monte Carlo sampling method to verify the SSD in 3D alignment combinations of horizontal curves in a cut section, where the cut side slope restricted the sight lines.

De Santos-Berbel and Castro [33] proposed a probabilistic approach to estimate the required SSD on a real highway, determining the most hazardous zones in terms of sight distance limitations, which were located at the tightest alignment elements. In another study, they compared different sight distance modelling methodologies including a 2D and two 3D methods, applied a reliability analysis to compute the P_{nc} of the SSD for each method, finding that the methods that overestimated the ASD underestimated P_{nc} [25].

Hussein *et al.* [5] applied reliability theory to calibrate geometric design models and produce guidelines with consistent levels of safety. In addition, Ismail and Sayed [34] evaluated the risk of deviating from the design requirements due to budgetary restrictions. They assessed the safety implications of deviating from the sight distance requirements in two real case studies. They also determined target P_{nc} values for the comparative evaluation of design.

In addition to sight distance related models, other geometric design parameters have been studied with reliability theory. Dhahir and Hassan [35] developed a probabilistic analysis to address the design of horizontal curves considering four criteria: vehicle stability, rollover, driver comfort and sight distance, in both dry and wet pavement conditions. Mollashahi *et al.* [36] proposed a method based on reliability theory to calibrate the superelevation in horizontal curves considering the operating speed. They found that the calibrated superelevation values were generally greater than those proposed by the American Association of State Highway and Transportation Officials (AASHTO) geometric design guide. Sarhan and Hassan [37] used the advantages of a probabilistic approach to develop a new methodology that calculates the required lateral clearance in 3D alignments. This reliability-based approach overcomes the shortcomings of the current design standard method when a non-vertical lateral obstruction limits the ASD in a horizontal curve overlapping with a vertical curve. Llorca *et al.* [38] developed a reliability analysis for passing sight distance based on the observation of maneuvers in a sample of two-lane Spanish roads. Ismail and Sayed [39] introduced a calibration framework for standard design models to determine a target safety value, applying the method to the design model of crest vertical curves.

Regarding the determination of P_{nc} with multiple failure modes, You *et al.* [40] performed a reliability analysis in horizontal curves for two failure modes: skidding and rollover of cars and trucks. To that end, they formulated a comparative study of 3 performance functions, calculating the P_{nc} of each vehicle type. In addition, Essa *et al.* [41] considered the failure modes of limited sight distance and vehicle skidding for the design of horizontal curves in a system reliability analysis.

Several tools to determine the P_{nc} have been developed. DAKOTA is an optimization software for the quantification of uncertainty in which the reliability analysis was implemented [42]. Moreover, Mahsuli and Haukaas [43] developed the Risk Tools (RT) software for reliability and optimization analysis. RT allows the use of multiple methodologies to provide probabilistic predictions of the actual performance of a civil infrastructure during its service life.

III. MATERIALS AND METHODS

This research study evaluates the probability of SSD exceeding the HSD on sag vertical curves that comply with the requirements of the Spanish geometric design standard [6]. To this end, several sag curves were generated on the basis of the design criteria.

Figure 1 outlines the research process prior to the calculation of P_{nc} based on reliability theory. Given that the LSF is defined as the difference between the HSD and the SSD, the variables on which the HSD and the SSD depend are described, including whether they are model parameters or random variables. In the case of the latter, the probability distributions must be characterized. The LSF features deter-

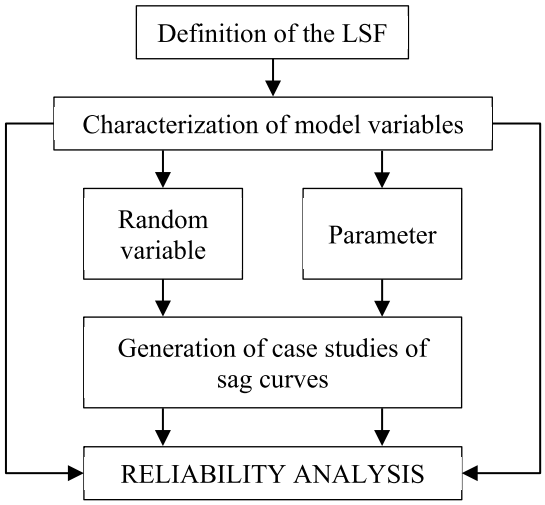

FIGURE 1. Research process prior to the reliability analysis.

mine the feasible reliability methods. Subsequently, all the admissible combinations, according to the Spanish standard, of the values of the variables defined as model parameters were generated resulting in the sample of sag vertical curves, which yielded 71,334 case studies. Then, the P_{nc} associated to each case was calculated using a reliability analysis tool (RT software) [43]. This computational process was automated through a MATLAB script.

A. LIMIT STATE FUNCTION

The LSF considered in the study, denoted by $g(x,\lambda)$ in (1), evaluated the difference between the supply (HSD) and the demand (SSD), where x is the input vector of random variables, and λ is the input vector of model parameters. When the value of the LSF is less than or equal to zero, the design is considered not to comply with the requirements.

$$g(x,\lambda) \leq 0 \Leftrightarrow \text{Noncompliance} \tag{1}$$

To assess the risk level (P_{nc}) associated with the limited sight distance in the sample of sag vertical curves, the HSD and the SSD were calculated for each case generated. The following sections describe in detail the process of these main parts.

1) HEADLIGHT SIGHT DISTANCE

The HSD was calculated analytically according to the geometry of the sag curve as well as the configuration of the headlight and the target. In this respect, the relation between the length of the sag vertical curve L and the position the furthest target visible when the vehicle headlights are located over the beginning of the sag curve must be taken into account since it determines the mathematical expression that evaluates the HSD. A sag vertical curve is considered as long if the furthest target visible is located within its limits (Figure 2a). Equation 2 was utilized in this case to calculate the HSD [44]. Otherwise, the sag vertical curve is considered as short

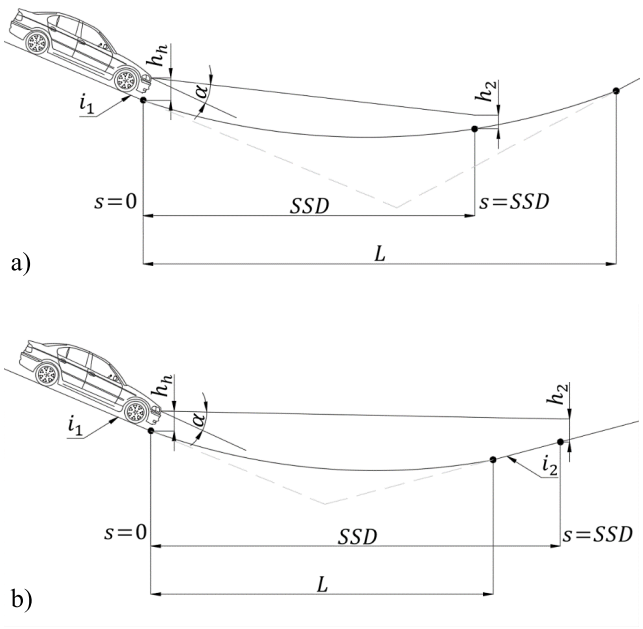

FIGURE 2. Schemas of sag vertical curves a) the HSD at the beginning is shorter than its length; b) the HSD at the beginning is larger than its length.

(Figure 2b), and the counterpart HSD is given by (3) [45].

If HSD $< L$

$$HSD \cong K_V \,.\, Tan\alpha \,.\, \left(1 + \sqrt{1 + 2 \,.\, \frac{h_h - h_2}{K_V \,.\, Tan\alpha}}\right) \tag{2}$$

If HSD $> L$

$$ASD \cong \frac{K_V \theta^2 + 2 \,.\, (h_h - h_2)}{2 \,.\, (\theta - Tan\alpha)} \tag{3}$$

where K_V is the rate of vertical curvature (m), α is the upward divergence angle of the headlamp beam, h_h is the headlamp height (m), h_2 is the target height (m), and θ is the algebraic difference between the inbound and outbound grades.

Each of the variables involved in (2) and (3) was treated either as a random variable or as a model parameter depending on the design considerations of the sag curves, the information available, and the effects to be analysed in the present study:

- *Absolute value of the algebraic difference between the inbound and outbound grades* (θ): This variable was treated as a model parameter as it is associated to the design of a sag curve. Its value is determined by the algebraic difference between the inbound and outbound grades (i_1 and i_2 respectively), which complied with the restrictions of the Spanish design standard as shown in Table 1.

- *Rate of vertical curvature* (K_V): This variable was treated as a model parameter as it is also associated to the design of a sag curve. The length of the vertical curve can be deduced as the product of K_V and θ. The values used were those specified by the design standard as detailed in Table 1.

TABLE 1. Characteristic values of the variables used in the model.

V_D (km/h)	σ_V (km/h)	V_{50} (km/h)	Min. i_1 (%)	Max. i_2 (%)	K_V (m)	$f_{l,95}$	σ_{fl}	$f_{l,50}$
40	6.878	32.872	-10.0	10.0	760	0.432	0.0805	0.5716
50	7.249	42.487	-10.0	10.0	1,160	0.411	0.0833	0.5556
60	7.759	51.958	-8.0	8.0	1,650	0.390	0.0844	0.5396
70	8.439	61.253	-8.0	8.0	2,300	0.369	0.0849	0.5240
80	9.328	70.333	-7.0	7.0	3,000	0.348	0.0858	0.5092
90	10.469	79.150	-7.0	7.0	3,800	0.334	0.0880	0.5020
100	11.911	87.655	-6.0	5.0	4,800	0.320	0.0925	0.4956
110	13.703	95.797	-6.0	5.0	5,900	0.306	0.1003	0.4919
120	15.893	103.528	-6.0	5.0	7,100	0.291	0.1123	0.4890
130	18.520	110.805	-6.0	5.0	8,600	0.277	0.1296	0.4890
140	21.611	117.601	-6.0	5.0	10,300	0.263	0.1531	0.4890

- *Upward angle of headlamp beam* (α): This variable was considered a model parameter as one of the objectives of this study is to disclose the possible impact of setting a smaller value of this angle in the standards on P_{nc}. Three values were utilized in this analysis: 1 degree as it is suggested in design standards [1], [6], and 0.75 and 0.9 degrees as suggested by Hawkins and Gogula [17].

- *Headlamp height* (h_h): The headlamp mounting height was incorporated as a random variable that followed a normal distribution to cover the existing variability in the different vehicles in the market. To characterize it, the data were derived from the 11 best-selling vehicles in Spain in 2015 [20]. The mean mounting height was 0.731 m and the standard deviation was 0.052 m.

- *Target height*(h_2): This variable was treated as a model parameter as one of the objectives of this study is to quantify the effect of considering different values of this height in the standards, which are discretionarily selected, on P_{nc}. The values assumed in this analysis were taken from the specifications of the Spanish geometric design standard [6], which states that the target height on the roadway surface must be set at 0.5 m, and a target height of not less than 0.2 m could be set on road sections where hazardous obstacles with a height less than 0.50 m might exist. Therefore, the target heights of 0.5 and 0.2 m were taken in the analysis.

2) STOPPING SIGHT DISTANCE

The SSD is the distance travelled by a vehicle forced to stop as quickly as possible. For its estimation, the equation of the Spanish geometric design standard [6] defined as follows was used:

$$SSD = \frac{V \cdot PRT}{3.6} + \frac{V^2}{254 \cdot (f_l + i)} \tag{4}$$

where V is the initial speed of the braking maneuver (km/h), PRT is the perception-reaction time (s), f_l is the longitudinal friction between the tyre and the pavement surface, and i is the longitudinal grade of the highway along the stopping maneuver.

The equation that estimates the SSD introduced additional variables in the system, which were characterized as follows:

- *Initial speed of the braking maneuver* (V): whereas the design speed (V_D) is typically considered for the calculation of the SSD; in this study, the speed was assumed as a random variable following a normal distribution. The set of input speed distributions used in this study was derived from the design speeds associated to the standardized sag vertical curve parameters, which are summarized in Table 1. However, in deterministic geometric design, the design speed corresponds to the 85-th percentile speed. Therefore, it is necessary to deduce the counterpart mean speed value (V_{50}) and standard deviation (σ_V) for the characterization of the speed as a random variable. For this purpose, the mathematical expressions of the operating speed model of Perez-Zuriaga [46] were adopted, which led to an equation that relates σ_V and V_{50} as follows:

$$\sigma_V = \sqrt{14.8194 + \exp\left(\frac{V_{50}^2 + 15760.216}{4841.26}\right)} \tag{5}$$

The values of the unknowns σ_V and V_{50} were derived from the design speed using equation (5) and the inverse normal distribution function. Their values are displayed in Table 1.

- *Perception-reaction time* (PRT): it was assumed that this was a random variable that followed a lognormal distribution. The values used to define this variable were taken from the results of the experiment conducted by Lerner [47]. The assumed values were a mean of 1.5 seconds and standard deviation of 0.4 seconds.

- *Tire-pavement longitudinal friction*(f_l): This variable was assumed to follow a random beta distribution, where the probability is conditioned by the speed. A distribution of this type is assumed instead of a normal distribution since the beta distribution takes values between 0 and 1 as opposed to the normal distribution, in which values greater than 1 and negative may appear, not meeting the physical phenomenon of longitudinal friction. In this sense, each value of the speed V_{50} was assumed to be associated with a beta distribution with its respective mean ($f_{l,50}$) and standard deviation (σ_{fl}) values. As occurred for the speed, a conservative percentile value of the longitudinal friction is considered in deterministic design. The Spanish standard provides 5-th percentile values of the longitudinal friction in relation to the design speed

as displayed in Table 1. To determine the standard deviation values σ_{fl} as a function of the speed, the relationship between longitudinal friction and speed by Bühlmann *et al.* [48] was adopted. The adjusted equation relating the speed V and the standard deviation of the longitudinal friction read:

$$\sigma_{fl} = 0.0343 + 2.2{\cdot}10^{-3} \cdot V - 3.2 \cdot 10^{-5} \cdot V^2 + 1.35 \cdot 10^{-5} \cdot V^3 \quad (6)$$

The adjusted values as per (6) are shown in Table 1, which are listed in relation to the design speed (V_D). Moreover, to define the series of random distribution of the longitudinal friction, the relationship between the mean values $f_{l,50}$ and the speed V must be defined. These values were deduced by applying the inverse beta distribution function to the $f_{l,95}$ values proposed by the standard. Then, the adjusted equation relating the speed V and the mean value of the longitudinal friction resulted:

$$f_{l,50} = 0.6673 + 2.8{\cdot}10^{-3} \cdot V - 1.1{\cdot}10^{-5} \cdot V^2 \quad (7)$$

The adjusted values obtained from (7) are also exhibited in Table 1, in relation to the design speed (V_D). The values obtained as per (6) and (7), distributed according to percentile values, are displayed in Figure 2. It can be observed that the friction decreases as the speed increases. This relation must be incorporated into the reliability analysis to achieve accurate results when computing the P_{nc} by means of the correlation coefficient between the speed and the longitudinal friction [43]. The correlation coefficient ρ can be calculated as follows:

$$\rho = \frac{\sigma_V \cdot \frac{df_{l,50}}{dV}}{\sigma_{fl}} \quad (8)$$

where ρ is the correlation coefficient between the speed and the mean value of the longitudinal friction. $(df_{l,50})$ / (dV) is the derivative of the longitudinal friction with respect to the speed, which can be deduced from (7). It must be noted that in the reliability analysis, equations (6), (7) and (8) were evaluated for the set of mean speeds V_{50}.

- *Highway grade along the stopping maneuver* (i): The values of this variable were incorporated into the reliability analysis in a way that depend on other model variables. On the one hand, it depends on the geometry of the sag curve, which is fundamentally determined by the parameters of the model. On the other hand, it depends on the SSD itself, thus producing a recursive dependence. Furthermore, as i is defined as the average grade along the stopping maneuver, the expression that determines its value varies depending on whether the vertical curve is long or short (Figure 2).

Sag vertical curves are geometrically defined by the equation of a second-degree parabola with vertical axis [44]:

$$z = z_0 + i_1 (s - s_0) + \frac{(s - s_0)^2}{2 \cdot K_V} \quad (9)$$

where z_0 is the height at the beginning of the sag vertical curve; s_0 is the distance from the origin to the beginning of the sag; s is the distance from the origin to a generic point and i_1 is the grade value of the inbound grade. Given that the average grade along the stopping maneuver is the grade of the straight line that connects the beginning of the sag and the point where stopping maneuver ends, its value be derived from (9) in the case where $L >$ SSD (Figure 2a) as follows:

$$i = i_1 + \frac{SSD}{2 \cdot K_V} \quad (10)$$

If $L <$ SSD (Figure 2b), the mathematical expression that determines the average grade along the stopping maneuver reads:

$$i = i_1 + \theta - \frac{K_V \cdot \theta^2}{2 \cdot SSD} \quad (11)$$

As seen in (4), (10) and (11), a recursive dependence indeed exists between the grade i and the SSD. A method of successive substitutions was used to approximate the values of both variables in the reliability analysis. Equation (4) and the piecewise function formed by (10) and (11) constitute a system of equations which can be expressed in compact form as follows:

$$\boldsymbol{X}_{k+1} = \boldsymbol{F}(\boldsymbol{X}_k) \quad k = 1, 2, 3 \ldots \quad (12)$$

where $\boldsymbol{X}_k$ is the vector that contains the value of the variables {SSD, i} at the k-th iteration, and $\boldsymbol{F}(\boldsymbol{X}_k)$ is the vector constituted by the above functions. The number of iterations necessary to reach convergence, namely until a smaller difference than desired between the outcome of two successive iterations was obtained, is defined by:

$$\|\boldsymbol{X}_{k+1} - \boldsymbol{X}_k\| < \boldsymbol{e_d} \quad (13)$$

where $\boldsymbol{e_d}$ is the convergence threshold vector. A value of 0.01 m was selected as convergence threshold for the variable SSD, which enabled the convergence with very few iterations while achieving the required precision.

B. SAMPLE GENERATION

Once characterized the model and its variables, a sample of sag vertical curves according to the Spanish geometric design standard was generated. The sample generation was associated to the design speeds and to the respective K_V values. For each K_V value, a set of possible combinations of inbound and outbound grades was generated. The grade values were generated at intervals of 0.25 %, and their combinations complied with a set of conditions. First, the outbound grade value was greater than the inbound grade value to produce sag vertical curves. Second, the inbound and outbound grades were enclosed within the maximum grade values allowed by the standard, including the exceptional increases, in relation to the corresponding design speeds (Table 1). In addition, the smaller grades included, in absolute value, were 0.25% since the minimum grade allowed in the design standard is 0.2%. Third, the combinations of inbound and outbound grades were to result in lengths equal to or greater than the

TABLE 2. Values adopted of model parameters for the hypotheses in HSD estimation.

Parameter	Values
α (°)	1.0, 0.9 and 0.75
h_2 (m)	0.5 and 0.2

counterpart design speed ($L \geq V_D$). The length of a sag curve is given by:

$$L = K_V * \theta \tag{14}$$

As a result, 11,889 sag curves were generated under these considerations.

Finally, each sag curve was to be examined under different assumptions concerning the values proposed for the parameters α and h_2 as detailed in section III.A.1. The six hypotheses resulting from the combinations of the values exhibited in Table 2 were assessed for each sag curve, which yielded a total of 71,334 case studies.

C. RELIABILITY ANALYSIS

The reliability analysis applied to sag vertical curves sought to assess the risk associated to sight distance limitations in nighttime. As mentioned earlier in this document, a LSF was applied, which in the context of this study, evaluated the difference between the supply (HSD) and the demand (SSD).

$$LSF = HSD - SSD \tag{15}$$

The HSD is determined as defined in section III.A.1, by means of equations (2) and (3) whereas the SSD is estimated with equation (4) as detailed in section III.A.2. In reliability theory, the P_{nc} is used to label the probability that a design output does not meet the standard, which occurs when the SSD exceeds the HSD.

In this study, the term of the LSF that refers to the supply (HSD) is modelled as per a piecewise function. Consequently, the LSF is not continuously differentiable, which makes the FORM, SORM and MVFOSM methods not suitable for the analysis [27]. Therefore, a sampling method was used to perform the reliability analysis.

To estimate the P_{nc} value several sampling schemes can be used. The simplest and most widely used approach is the Monte Carlo method [49]. Monte Carlo is a repeated random sampling method utilized to obtain an approximate solution.

The results obtained by the simulation carried out using the Monte Carlo method unavoidably entail sampling errors, which decrease as the sample size increases. Therefore, one way to avoid sampling errors is to increase the sample size.

The P_{nc} in this method is determined by the following equation [24]:

$$P_{nc} = \frac{N_{pu}}{N} \tag{16}$$

where N_{pu}Npu is the number of unsatisfactory performances, and N is the number of Monte Carlo iterations.

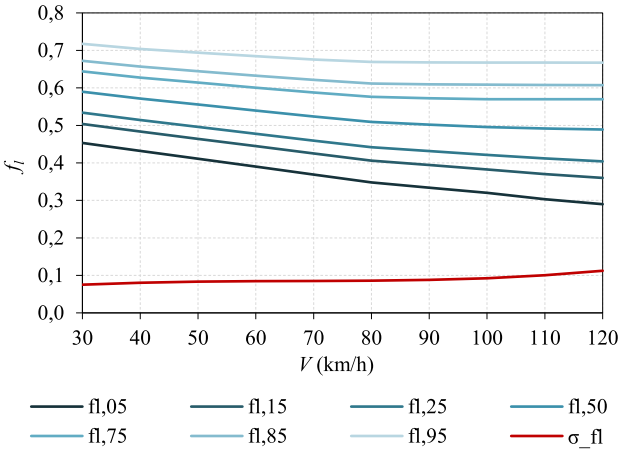

FIGURE 3. Adjusted longitudinal friction distributions as a function of the speed.

In order to achieve enough accuracy in sampling, the coefficient of variation of the successive P_{nc} values during the Monte Carlo iteration was monitored:

$$\delta_{P_{nc}} = \frac{\sigma_{P_{nc}}}{\mu_{P_{nc}}} \tag{17}$$

where δ_{Pnc} is the coefficient of variation of P_{nc}, σ_{Pnc} is the standard deviation of P_{nc}, and μ_{Pnc} is the mean value of P_{nc}. Values of the coefficient of variation around 2-5% are considered as acceptable [49]. In this analysis, a value of 5% was adopted to guarantee the accuracy of the sampling.

RT software was selected to perform the reliability analysis and compute the P_{nc} [41]. The program can perform the reliability analysis through the Monte Carlo sampling method. The LSF was implemented in a JavaScript subroutine in order be able to compute it with successive substitutions. For each of the 71,334 case studies, the program generated a vector of random variables, each one extracted from its counterpart random distribution, and checked the compliance of the LSF. This process was iterated until the target coefficient of variation was obtained, or up to 100,000 iterations if otherwise. The computation was automated by means of a MATLAB script. Figure 4 shows a flowchart of the P_{nc} calculation process in RT.

IV. RESULTS AND DISCUSSION

As mentioned above, the 71,334 case studies generated can be classified into 6 groups according to the possible combinations of the values of the parameters α and h_2 shown in Table 2 in order to analyse the effect of these parameters on the P_{nc}.

Figure 5 displays four box-and-whisker plots that represent the ranges of P_{nc} values observed, grouped according to the K_V values and to the assumed values of the model parameters α and h_2. The lower and upper extreme of whiskers indicate the maximum and minimum P_{nc} values, and the boxes represent the intermediate quartiles for the specified values of K_V, α and h_2.

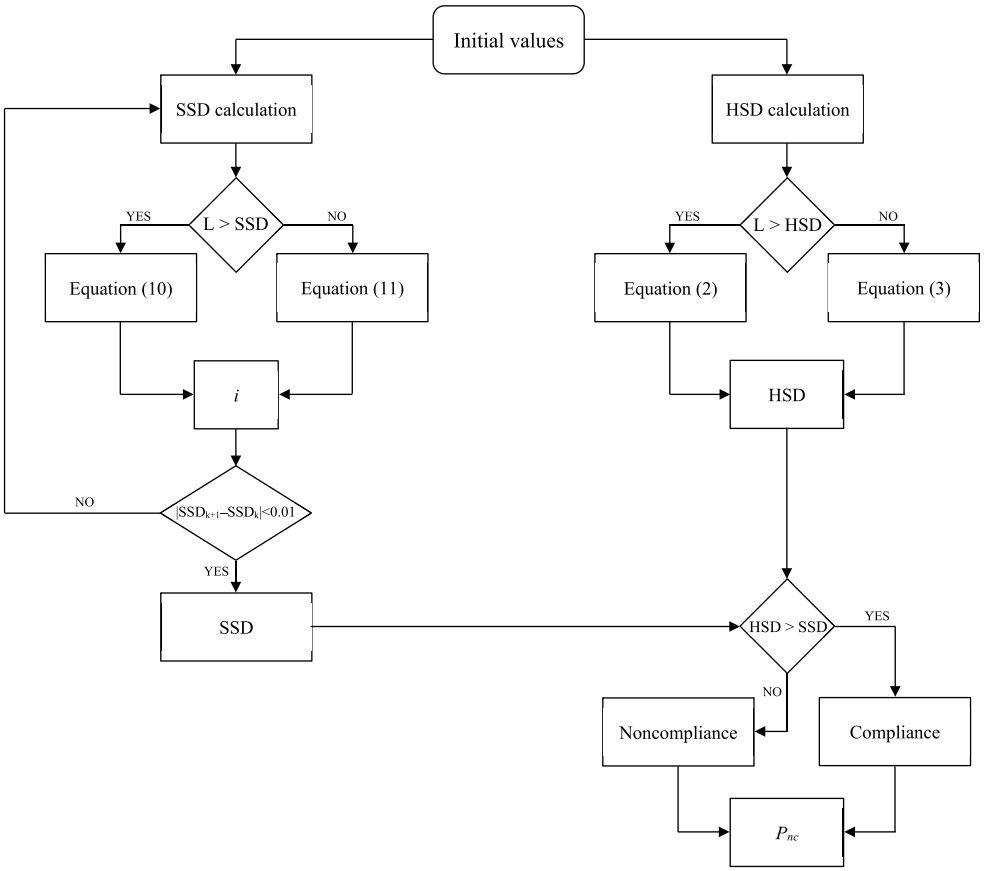

FIGURE 4. Flowchart of the calculation process of P_{nc} in RT.

Figure 5a examines the global effect of the target height h_2 on P_{nc} values as the data plotted include all the assumed values of the parameter α. It can be observed that the P_{nc} values significantly decrease as the K_V values increase for $h_2 = 0.5$ m, whereas the P_{nc} values slightly increase as the K_V values increase for $h_2 = 0.2$ m. The former result is consistent with the design standard since greater K_V values are associated with higher design speeds, where higher safety performance must be better and, therefore, P_{nc} must be smaller. However, the case studies where $h_2 = 0.2$ m was considered, did not show such a consistent pattern. In addition, the P_{nc} values of the case studies in which h_2 was set at 0.5 m were significantly higher than those where it was 0.2 m. This occurred because the increase in h_2 produces a reduction of the HSD on sag curves. Hence the evaluation of the difference between this reduced HSD and the SSD produced an increase in the P_{nc}. Furthermore, the range of P_{nc} values decreased as the K_V value increased. This occurred because greater algebraic differences between grades are allowed by the standard, thus producing more dispersion of the P_{nc} values.

Figure 5b illustrates the global effect of the angle α on P_{nc} values including all the assumed values of the target height h_2. The results showed that the P_{nc} values became closer to zero as the K_V value increased, regardless of the value of the angle α. In addition, for a given value of K_V, the ranges of P_{nc} values were closer to zero for greater values of the angle α. This effect is produced because the decrease of α when the rest of the parameters are kept constant produced a reduction of the HSD, which yielded a higher P_{nc} value when compared to the SSD values.

The effect of the target height h_2 on P_{nc} values when the angle α was set at 1° is displayed in Figure 5c. When the target height remained at 0.5 m, the P_{nc} values decreased as the value of K_V increased. It must be highlighted that these series correspond to the values proposed by the current Spanish design standard. This decrease was steadier than that produced in the complete sample. However, when the target height was set at 0.2 m, the ranges of P_{nc} values hardly varied for the different K_V values. Another noteworthy finding is that the differences between the ranges of P_{nc} values of the two target heights showed more significant differences for smaller K_V values than in the complete sample.

Figure 5d exhibits the effect of the angle α when the target height was set at 0.5 m. It can be noticed that the P_{nc} values decreased as the K_V values increase as occurred in the complete sample. Nevertheless, the ranges of P_{nc} presented greater differences between the three values assumed of the angle α than those existing in the complete sample. It was also found that the series in which the angle α was set at 1°

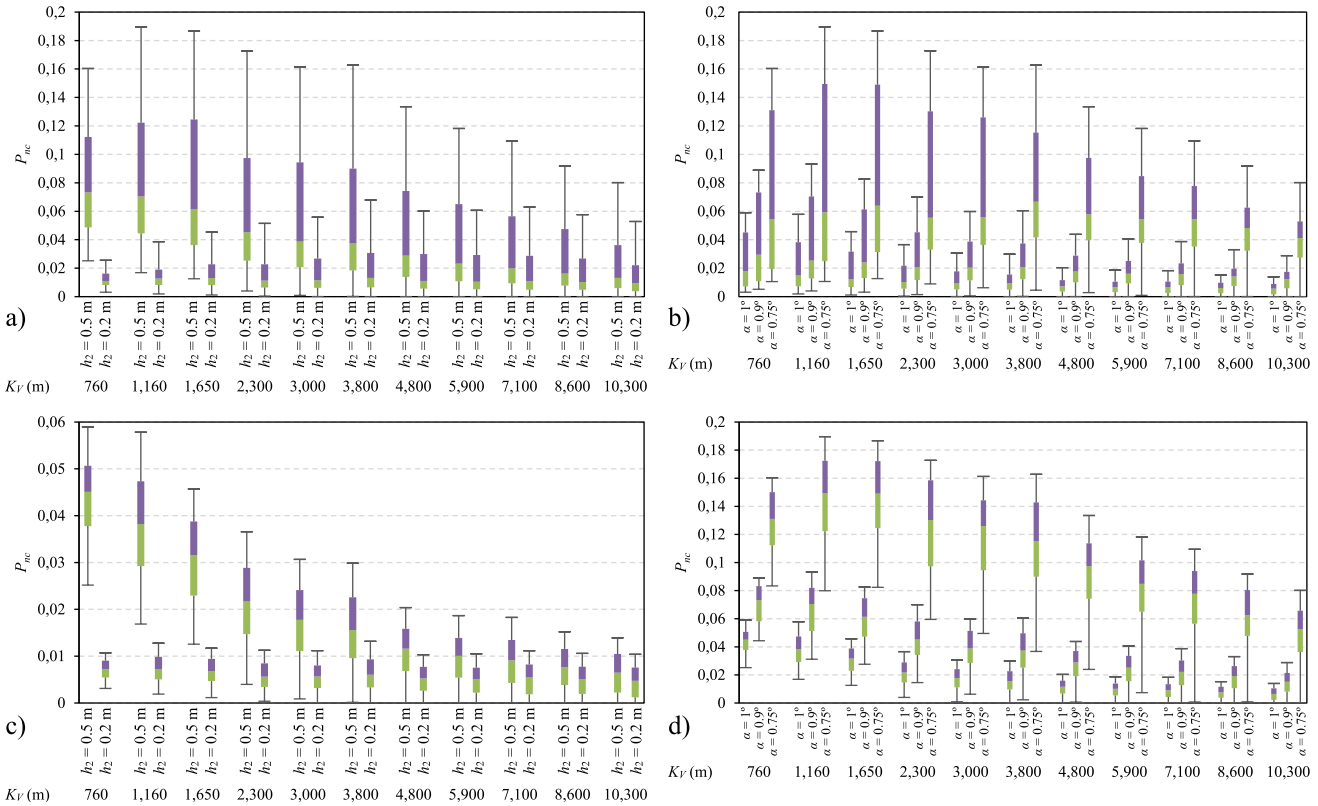

FIGURE 5. Ranges of P_{nc} values for each K_V value: a) effect of h_2 on the complete sample; b) effect of α on the complete sample; c) effect of h_2 for $\alpha = 1°$; and d) effect of α for $h_2 = 0.5$ m.

(values proposed by the current Spanish design standard) showed the lowest P_{nc} values.

Overall, the case studies where a target height of 0.2 m and an angle α of 1° were assumed had the lowest P_{nc} values for a given K_V, which represent the least conservative criteria in the design of sag curves. However, as aforementioned, previous research showed the need to revise sag curve design criteria concerning the value of the angle α [16], [17].

After analyzing the effect of the angle α and the target height h_2 on the P_{nc} values, the effects of the inbound and outbound grades (i_1 and i_2 respectively) as well as the algebraic difference between them (θ) on P_{nc} were studied.

Figure 6a represents the P_{nc} values obtained for three selected values of the parameter K_V in relation to the inbound grade value i_1, in which the angle α was 1° and the target height h_2 was 0.5 m as required by the Spanish standard. In the series where K_V was 760 m, the P_{nc} values decreased as the value of the inbound grade i_1 increase. A unique P_{nc} value is associated to each value of i_1. In the series where K_V was 1,650 m, the P_{nc} values also decreased as the value of the inbound grade i_1 increase. However, more than one value is associated to each value of i_1, which indicates that P_{nc} depends also on the value of θ. If the series where K_V was 5,900 m are observed, it can be noticed that the decreasing trend of P_{nc} was maintained whereas a greater dependence on the θ value was found.

Figure 6b displays the P_{nc} values that resulted when the K_V was 5,900 m plotted in relation to the value of the parameter θ. It demonstrates that P_{nc} varied not only depending on i_1 but also on θ. The only exception is the series of $\theta = 0.02$, where all the design outputs are associated to zero P_{nc}. This is produced due to the long distance lit up by the headlamps on the outbound grade where the parameter θ had a reduced value.

The P_{nc} values obtained for same three K_V values are illustrated in Figure 7a in relation to the outbound grade value i_2. The values of the angle α and the target height h_2 assumed were likewise those specified in the Spanish design standard. The dispersion of P_{nc} values for each series is greater than when the data was plotted according to the value of the inbound grade i_1, particularly for $K_V = 760$ m. This confirms the preponderance of the impact of the inbound grade i_1 over the outbound grade value i_2 on P_{nc}. It must be noted that the boundaries of the areas covered by the points are a consequence of the restrictions of the standard to the values of i_1, i_2 and L.

Figure 7b shows the P_{nc} values in the sag designs in which K_V was 5,900 m, distinguishing the values of the inbound grade i_1. For the lowest values of the grade i_2, it has a considerable impact on P_{nc} is very high. From a given point, which is different for each series, the effect is virtually nonexistent. It can be hence concluded that the relationship between i_2 and P_{nc} is markedly non-linear.

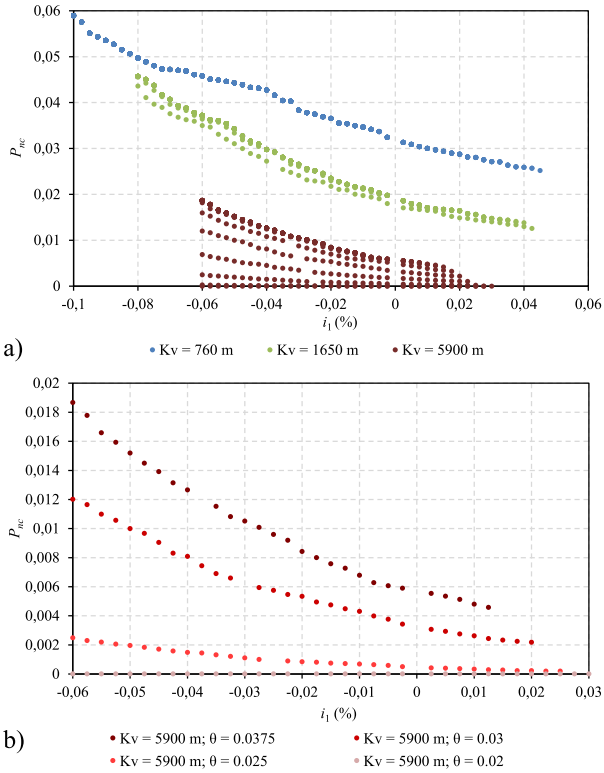

FIGURE 6. Scatter plot of P_{nc} in relation to i_1: a) various K_V values; and b) dependence on θ for $K_V = 5,900$ m.

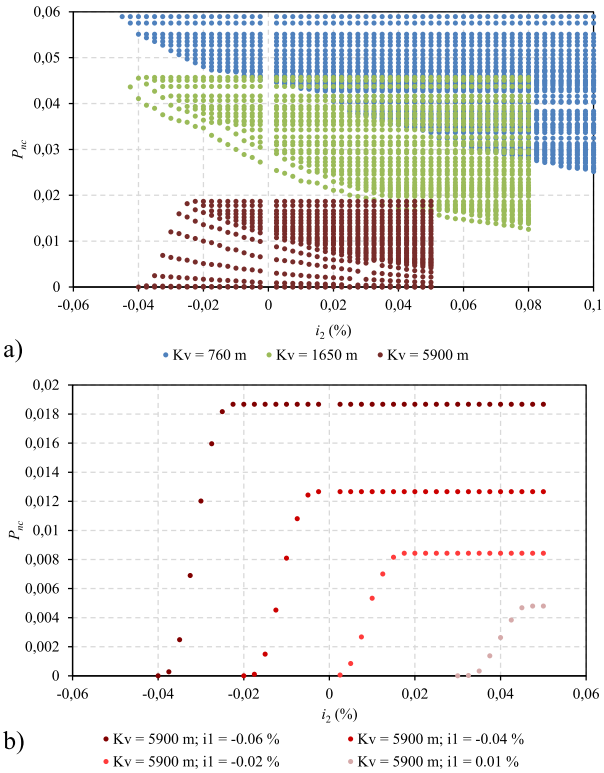

FIGURE 7. Scatter plot of P_{nc} in relation to i_2: a) various K_V values; and b) dependence on i_1 for $K_V = 5,900$ m.

Figure 8a shows the P_{nc} values as a function of the input θ values for $K_V = 5,900$ m. The minimum and maximum inbound and outbound grades respectively allowed by the

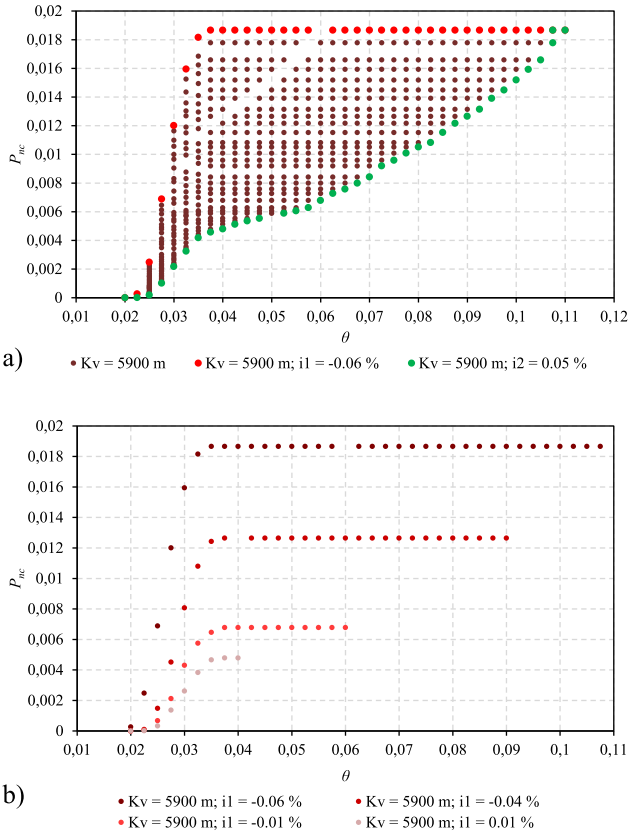

FIGURE 8. Scatter plot of P_{nc} in relation to θ for $K_V = 5,900$ m: a) all P_{nc} values; and b) dependence on i_1.

standard ($i_1 = -0.06$ and $i_2 = 0.05$ %) are highlighted. It can be noticed that the lowest P_{nc} values are produced for the lowest values of i_1, i_2 and θ. The reason behind this finding is that small θ values enable long HSD, which produce low P_{nc} values in comparison to the SSD, where the impact of i is minimum.

Figure 8b illustrates the P_{nc} values in series according to the inbound grade value i_1. The same non-linear relation between P_{nc} and θ as is Figure 7b is noticeable, being i_1 the parameter that determines the P_{nc} value. Nevertheless, the value of θ at which it ceases to have effect remains virtually constant at 0.0375 for all i_1 values. This finding occurred for all P_{nc} series, and the threshold θ values ranged from 0.055 (for $K_V = 760$ m) to 0.035 (for $K_V = 10,300$ m).

V. CONCLUSIONS

In this research study, the potential effect of geometric parameters that determine the design of sag vertical curves on road safety was studied using a probabilistic approach. The LSF evaluated the difference between the HSD and the SSD through reliability theory. Given the particularities existing in the LSF, a Monte Carlo method was selected to compute the P_{nc} associated to 11,889 cases of sag curves. The variables involved were characterized and considered as model parameters or random accordingly. Six combinations of model parameters were contemplated in the evaluation.

First, the effect of the model parameters α and h_2 was assessed. The consideration of a smaller vertical spread angle α produced a reduction of the HSD, which significantly increased the P_{nc} value when compared to the SSD. In addition, the increase of the target height h_2 produced a decrease of the HSD, which increased the P_{nc} values. When analysing the value proposed by design standards for the angle α, it can be noticed that a spread angle of 1°, low P_{nc} values were obtained in comparison to the results when more restrictive criteria found in literature were applied. In fact, the actual values of the angle α in vehicle frontlighting systems have been acknowledged not to emit enough light over 1° above the headlamp axle. Hence the current criterion might produce an overestimation of the safety performance.

Concerning the values of the target height h_2, the use of 0.5 m as input yielded significantly higher P_{nc} than those of the value 0.2. As a result, the combined effect of considering a reduced angle α and a higher h_2 in sag curve design, which represents the most conservative hypothesis, produced a very significant increase of the P_{nc} values. On the contrary, when α was set at 1° and h_2 at 0.2 m, the lowest P_{nc} values were obtained.

Regarding the rate of vertical curvature K_V, the observed effect on P_{nc} differed depending on the model parameters assumed. Under the assumptions of the Spanish design standard ($\alpha = 1°$ and $h_2 = 0.5$ m) greater K_V values yielded design outputs associated to lower risk levels. This consistent result was, nonetheless, not observed if, for example a reduced target height was used ($h_2 = 0.2$m).

As estimated in this research, the grade i along the simulated stopping maneuvers depended on the inbound and outbound grades of the sag (i_1 and i_2 respectively) as well as the curvature rate K_V. As evidenced by the results, the impact of the inbound grade i_1 on P_{nc} is very significant since it determines the highest P_{nc} value for a given K_V. Moreover, for the smallest K_V values such as 760 m and 1,160 m, the P_{nc} values did not depend on the outbound grade value i_2. Given the potential impact of the inbound grade i_1 on safety, its incorporation into sag curve design models is highly recommended. The outbound grade value was also found to affect P_{nc}. In addition, it was observed that P_{nc} reached a maximum value when a certain value of the algebraic difference between grades (θ) was exceeded for each value of i_1, and it did not depend on i_2 nor θ. These variables should also be contemplated for the design of sag vertical curves, since their variation affected the P_{nc} output, potentially producing different safety performance. Indeed, two sag curves featured with the same K_V and different i_1 are considered to have an equivalent level of safety from the point of view of the design standard, while this study showed that the variation of i_1 affects the expected safety performance.

To incorporate adequately the effect of each of the variables involved, the use of reliability theory is recommended in the development of geometric design standards and guides, and particularly for sag vertical curves. Moreover, the effect of i_1 and θ should also be considered in the design of a sag vertical curve in addition to the parameter K_V. Although the present study focused on the Spanish standard, the conclusions can be extrapolated to other countries since the findings might not be expected to change from a qualitative point of view. However, the random variables of the model should be calibrated to adapt the model to the country where it is to be implemented.

As future lines of research, the calibration of geometric design models is proposed to obtain consistent levels of safety, as well as to develop a methodology that establishes target P_{nc} values based on safety performance. In addition, the analysis of HSD on 3D alignments by means of a probabilistic approach is proposed.

REFERENCES

[1] AASHTO, *A Policy on Geometric Design of Highways and Streets 2018*, 7th ed. Washington, DC, USA: American Association of State Highway and Transportation Officials (AASHTO), 2018.
[2] RACE. (2013). *La visión En La Conducción Nocturna*. Accessed: 12-May 12, 2019. [Online]. Available: https://www.race.es/vision-y-conduccion-nocturna
[3] DGT, *Las Principales Cifras De La Siniestralidad Vial. Edición Ampliada. España 2017*, Directorate-Gen. Traffic, Madrid, Spain, 2017.
[4] K. Ismail and T. Sayed, "Risk-optimal highway design: Methodology and case studies," *Saf. Sci.*, vol. 50, no. 7, pp. 1513–1521, Aug. 2012.
[5] M. Hussein, T. Sayed, K. Ismail, and A. Van Espen, "Calibrating road design guides using risk-based reliability analysis," *J. Transp. Eng.*, vol. 140, no. 9, Sep. 2014, Art. no. 04014041.
[6] Ministerio de Fomento, *Norma 3.1 IC—Instrucción de Carreteras: Trazado*. Madrid, Spain: Ministerio de Fomento, 2016.
[7] B. Adler and H. Lunenfeld, "Three beam headlight evaluation," Nat. Highway Traffic Saf. Admin., U.S. Dept. Transp., Washington, DC, USA, Tech. Rep. DOT/HS-800-844, 1973.
[8] T. Åkerstedt, G. Kecklund, and L.-G. Hörte, "Night driving, season, and the risk of highway accidents," *Sleep*, vol. 24, no. 4, pp. 401–406, Jun. 2001.
[9] S. Gaca and M. Kiec, "Influence of night-time lighting restrictions on road design," in *Proc. 5th Int. Symp. Highway Geometric Design*, 2015.
[10] S. Papadimitriou and B. Psarianos, "Sight distance analysis on dry pavement during nighttime addressing wildlife crashes on two-lane rural roads," *Adv. Transp. Stud. Int. J. A*, vol. 35, pp. 5–18, Apr. 2015.
[11] S. Lee and Y. Kim, "Sight distance for a headlamp-only illumination condition," in *Proc. 5th Int. Symp. Highway Geometric Design*, 2015.
[12] K. M. Bauer and D. W. Harwood, "Safety effects of horizontal curve and grade combinations on rural two-lane highways," *Transp. Res. Rec., J. Transp. Res. Board*, vol. 2398, no. 1, pp. 37–49, Jan. 2013.
[13] C. M. Noble, B. Marsh, and A. Lauer, "Thoughts on highway design research as related to safety of vehicle operation," *Highway Res. Board Proc.*, vol. 17, Dec. 1937.
[14] W. C. Giessler, "The relationship of headlamps to road speeds," Illinois Div. Highway, Springfield, IL, USA, 1937.
[15] AASHO, *A Policy on Geometric Design of Rural Highways*. Washington, DC, USA: American Association of State Highway Officials (AASHO), 1954.
[16] R. B. Gibbons, A. Medina, B. Williams, J. Du, and H. Rakha, *Sag Vertical Curve Design Criteria for Headlight Sight Distance*. Washington, DC, USA: National Cooperative Highway Research Program, Transportation Research Board, 2012.
[17] H. Gene Hawkins and M. Gogula, "Assessment of sag curve design criteria considering modern headlamp performance," *Transp. Res. Rec., J. Transp. Res. Board*, vol. 2060, no. 1, pp. 3–9, Jan. 2008.
[18] S. M. Easa and Y. Hassan, "Headlight sight distance on separate highway alignments: A new approach," *Can. J. Civil Eng.*, vol. 24, no. 6, pp. 1007–1018, 1997.
[19] Y. Hassan, S. M. Easa, and A. O. Abd El Halim, "Modeling headlight sight distance on three-dimensional highway alignments," *Transp. Res. Rec., J. Transp. Res. Board*, vol. 1579, no. 1, pp. 79–88, Jan. 1997.

[20] C. De Santos-Berbel, M. Castro, and L. Iglesias, "Influence of headlamp lighting parameters on nighttime sight distance," in *Proc. 3rd Int. Conf. Traffic Transp. Eng. (ICTTE)*, 2016, pp. 88–94.
[21] C. De Santos-Berbel and M. Castro, "Effect of vehicle swiveling headlamps and highway geometric design on nighttime sight distance," *Math. Comput. Simul.*, vol. 170, pp. 32–50, Apr. 2020.
[22] Q. Zhang, R. Kang, and M. Wen, "Decomposition method for belief reliability analysis of complex uncertain random systems," *IEEE Access*, vol. 7, pp. 132711–132719, 2019.
[23] L. Shen, H. Shao, C. Li, W. Sun, and F. Shao, "Modeling stochastic overload delay in areliability-based transit assignmentmodel," *IEEE Access*, vol. 7, pp. 3525–3533, 2019.
[24] A. Musunuru, R. J. Porter, T. Sayed, and M. Fyfe, "Risk and reliability analysis of geometric design criteria: A critical synthesis," *Transp. Res. Rec., J. Transp. Res. Board*, vol. 2673, no. 3, pp. 386–398, Mar. 2019.
[25] C. de Santos-Berbel, M. Essa, T. Sayed, and M. Castro, "Reliability-based analysis of sight distance modelling for traffic safety," *J. Adv. Transp.*, vol. 2017, pp. 1–12, May 2017.
[26] X. Chai, Z. Sun, J. Wang, Y. Zhang, and Z. Yu, "A new kriging-based learning function for reliability analysis and its application to fatigue crack reliability," *IEEE Access*, vol. 7, pp. 122811–122819, 2019.
[27] T. Haukaas. (2019). *Notes of MVFOSM, FORM, SOSM*. Accessed: Jul. 8, 2019. [Online]. Available: http://civil-terje.sites.olt.ubc.ca/files/2019/06/MVFOSM-FORM-SORM.pdf
[28] J. Santos del Cerro and M. García Secades, *Historia de la Probabilidad y la Estadística (III)*. Madrid, Spain: Delta, 2006.
[29] F. P. D. Navin, "Safety factors for road design: Can they be estimated?" *Transp. Res. Rec.*, vol. 1280, no. 1280, pp. 181–189, 1990.
[30] F. P. D. Navin, "Reliability indices for road geometric design," *Can. J. Civil Eng.*, vol. 19, no. 5, pp. 760–766, Oct. 1992.
[31] L. Richl and T. Sayed, "Evaluating the Safety Risk of Narrow Medians," *J. Transp. Eng.*, vol. 132, no. 5, pp. 366–375, 2006.
[32] M. Sarhan and Y. Hassan, "Three-dimensional, probabilistic highway design: Sight distance application," *Transp. Res. Rec., J. Transp. Res. Board*, vol. 2060, no. 1, pp. 10–18, Jan. 2008.
[33] C. De Santos-Berbel and M. Castro, "Stopping-sight-distance simulation using a new probabilistic approach," in *Proc. 5th Int. Symp. Highway Geometric Design*, 2015.
[34] K. Ismail and T. Sayed, "Risk-based highway design: Case studies from British Columbia, Canada," *Transp. Res. Rec., J. Transp. Res. Board*, vol. 2195, no. 1, pp. 3–13, Jan. 2010.
[35] B. Dhahir and Y. Hassan, "Probabilistic, safety-explicit design of horizontal curves on two-lane rural highways based on reliability analysis of naturalistic driving data," *Accident Anal. Prevention*, vol. 123, pp. 200–210, Feb. 2019.
[36] H. F. Mollashahi, K. Khajavi, and A. K. Ghaeini, "Safety evaluation and adjustment of superelevation design guides for horizontal curves based on reliability analysis," *J. Transp. Eng., A, Syst.*, vol. 143, no. 6, Jun. 2017, Art. no. 04017013.
[37] M. Sarhan and Y. Hassan, "Reliability-based methodology to calculate lateral clearance on three-dimensional alignment," in *Proc. 88th Annu. Meeting Transp. Res. Board*, 2009.
[38] C. Llorca, A. T. Moreno, T. Sayed, and A. García, "Sight distance standards based on observational data risk evaluation of passing," *Transp. Res. Rec., J. Transp. Res. Board*, vol. 2404, no. 1, pp. 18–26, Jan. 2014.
[39] K. Ismail and T. Sayed, "Risk-based framework for accommodating uncertainty in highway geometric design," *Can. J. Civil Eng.*, vol. 36, no. 5, pp. 743–753, May 2009.
[40] K. You, L. Sun, and W. Gu, "Reliability-based risk analysis of roadway horizontal curves," *J. Transp. Eng.*, vol. 138, no. 8, pp. 1071–1081, Aug. 2012.
[41] M. Essa, T. Sayed, and M. Hussein, "Multi-mode reliability-based design of horizontal curves," *Accident Anal. Prevention*, vol. 93, pp. 124–134, Aug. 2016.
[42] S. N. Laboratories. (2017). *DAKOTA, Explore and Predict With Confidence*. Accessed: Aug. 22, 2019. [Online]. Available: https://dakota.sandia.gov/
[43] M. Mahsuli and T. Haukaas, "Computer program for multimodel reliability and optimization analysis," *J. Comput. Civil Eng.*, vol. 27, no. 1, pp. 87–98, Jan. 2013.
[44] C. Kraemer, J. M. Pardillo, S. Rocci, M. Romana, V. Sanchez, and M. A. del Val, *Ingenieria de Carreteras*, 2nd ed. Madrid, Spain: McGraw-Hill, 2009.
[45] C. Kraemer, S. Rocci, and V. Sanchez, *Trazado de Carreteras*, 2nd ed. Madrid, Spain: Escuela Tecnica Superior de Ingenieros de Caminos, Canales y Puertos de Madrid, 1992.
[46] A. M. Pérez Zuriaga, "Caracterización y modelización de la velocidad de operación en carreteras convencionales a partir de la observación naturalística de la evolución de vehículos ligeros," Ph.D. dissertation, Univ. Politècnica de Valencia, Valencia, Spain, 2012.
[47] N. Lerner, "Age and driver perception-reaction time for sight distance design requirements," in *Proc. Compendium Tech. Papers. Inst. Transp. Eng. 65th Annu. Meeting. Inst. Transp. Eng. (ITE)*, 1995, pp. 624–628.
[48] F. Bühlmann, H. P. Lindenmann, and P. Spacek, *Sichtweiten Überprüfen Der Grundlagen Zur VSS-Norm SN 640 090 Projektierungsgrundlagen, Sichtweiten*. Zürich, Switzerland: Institut für Verkehrsplanung und Transporttechnik, Strassen-und Eisenbahnbau, 1991.
[49] T. Haukaas. (2019). *Notes of Sampling*. Accessed: Jul. 8, 2019. [Online]. Available: http://civil-terje.sites.olt.ubc.ca/files/2019/06/Sampling.pdf